ELSEVIER

Landmark constrained genus zero surface conformal mapping and its application to brain mapping research

Lok Ming Lui [a], Yalin Wang [a,*], Tony F. Chan [a], Paul Thompson [b]

[a] *Department of Mathematics, UCLA, Los Angeles, CA 90095-1555, USA*
[b] *Laboratory of Neuro Imaging and Brain Research Institute, UCLA School of Medicine, CA 90095-1555, USA*

Abstract

In order to compare and integrate brain data more effectively, data from multiple subjects are typically mapped into a canonical space. One method to do this is to conformally map cortical surfaces to the sphere. It is well known that any genus zero Riemann surface can be mapped conformally to a sphere. Cortical surface is a genus zero surface. Therefore, conformal mapping offers a convenient method to parameterize cortical surfaces without angular distortion, generating an orthogonal grid on the cortex that locally preserves the metric. Although conformal mapping preserves the local geometry well, the important anatomical features, such as the sulci landmarks, are usually not aligned consistently. To compare cortical surfaces more effectively, it is advantageous to adjust the conformal parameterizations to match consistent anatomical features across subjects. This matching of cortical patterns improves the alignment of data across subjects, although it is more challenging to create a consistent conformal (orthogonal) parameterization of anatomy across subjects when landmarks are constrained to lie at specific locations in the spherical parameter space. Here we describe two methods to accomplish the task. The first approach is based on pursuing an optimal Möbius transformation to minimize the landmark mismatch error. The second approach is based on a new energy functional, to optimize the conformal parameterization of cortical surfaces by using landmarks. Experimental results on a dataset of 40 brain hemispheres showed that the landmark mismatch energy can be significantly reduced while effectively preserving conformality. The key advantage of these conformal parameterization approaches is that any local adjustments of the mapping to match landmarks do not affect the conformality of the mapping significantly. A detailed comparison between the two approaches will be discussed. The first approach can generate a map which is exactly conformal, although the landmark mismatch error is not reduced as effective as the second approach. The second approach can generate a map which significantly reduces the landmark mismatch error, but some conformality will be lost.

1. Introduction

Rapid development of computer technology has accelerated the acquisition and databasing of brain data. An effective way to analyze and compare brain data from multiple subjects is to map them into a canonical space while retaining the original geometric information as far as possible. Surface-based approaches often map cortical surface

---

* Corresponding author.
  E-mail addresses: malmlui@math.ucla.edu (L.M. Lui), ylwang@math.ucla.edu (Y. Wang), tonyc@math.ucla.edu (T.F. Chan),
thompson@loni.ucla.edu (P. Thompson).
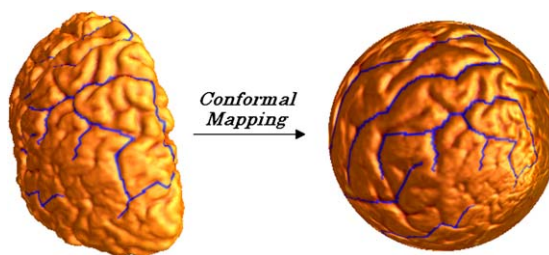
Fig. 1. Manually labeled landmarks on the brain surface. The original surface is on the left. Its conformal mapping result to a sphere is on the right.

data to a parameter domain such as a sphere, providing a common coordinate system for data integration [1,2]. One method is to map the cortical surface conformally to the sphere. Any genus zero Riemann surfaces can be mapped conformally to a sphere, without angular distortion. Therefore, conformal mapping offers a convenient way to parameterize the genus zero cortical surfaces of the brain. To compare cortical surfaces more effectively, it is desirable to adjust the conformal parameterizations to match specific anatomical features on the cortical surfaces as far as possible (such as sulcal/gyral landmarks in the form of landmark points or 3D curves lying in the surface). Here we refer to these anatomical features as landmarks. Some examples of landmarks are shown in Fig. 1.

1.1. Previous work

Several research groups have reported work on brain surface conformal mapping. Hurdal and Stephenson [6] reported a discrete mapping approach that uses circle packing to produce "flattened" images of cortical surfaces on the sphere, the Euclidean plane, or the hyperbolic plane. They obtained maps that are quasi-conformal approximations to classical conformal maps. Haker et al. [5] implemented a finite element approximation for parameterizing brain surfaces via conformal mappings. They represented the Laplace–Beltrami operator as a linear system and solved it for parameterizing brain surfaces via conformal mapping. Timsari et al. [10] proposed a method for creating semi-isometric flat maps of sections of the human cortical surface. They have formulated the calculation of an isometric mapping between surfaces as a constrained optimization problem. Gu et al. [4] proposed a method to find a unique conformal mapping between any two genus zero manifolds by minimizing the harmonic energy of the map. They demonstrated this method by conformally mapping the cortical surface to a sphere. For general surfaces, Wang et al. [12] proposed a method to compute the conformal structures of high genus surfaces using the holomorphic 1-forms. They illustrated this ideas by computing conformal structures for several types of anatomical surfaces in MRI scans of the brain, including the cortex, hippocampus, and lateral ventricles. Based on the Riemann surface structure, they then canonically partitioned the surface into patches and each of these patches can be conformally mapped to a parallelogram.

Optimization of surface diffeomorphisms by landmark matching has been studied intensively. Gu et al. [4] proposed to optimize the conformal parametrization by composing an optimal Möbius transformation so that it minimizes the landmark mismatch energy. The resulting parameterization remains conformal. Joan et al. [3] proposed to generate large deformation diffeomorphisms of the sphere onto itself, given the displacements of a finite set of template landmarks. The diffeomorphism obtained can match the geometric features significantly but it is, in general, not a conformal mapping. Leow et al. [7] proposed a level set based approach for matching different types of features, including points and 2D or 3D curves represented as implicit functions. Cortical surfaces were flattened to the unit square. Nine sulcal curves were chosen and were represented by the intersection of two level set functions, and used to constrain the warp of one cortical surface onto another. The resulting transformation was interpolated using a large deformation momentum formulation in the cortical parameter space, generalizing an elastic approach for cortical matching developed in Thompson et al. [9]. Duygu et al. [11] proposed a more automated mapping technique that results in good sulcal alignment across subjects, by combining parametric relaxation, iterated closest point registration and inverse stereographic projection.

2. Basic mathematical theory

A diffeomorphism $f : M \to N$ is a *conformal mapping* if it preserves the first fundamental form up to a scaling factor (the conformal factor). Mathematically, this means that $ds_M^2 = \lambda f^*(ds_N^2)$, where ds_M^2 and ds_N^2 are the first
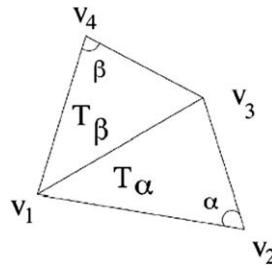
Fig. 2. Discrete Laplace–Beltrami operator. Edge $\{v_1, v_2\}$ has two corners against it α, β The edge weight is defined as the summation of the cotangents of these corner angles.

fundamental form on M and N, respectively and λ is the conformal factor. For a diffeomorphism between two genus zero surfaces, a map is conformal if it minimizes the harmonic energy,[1] E_{harmonic} [1]. Based on this fact, we can compute the conformal mapping by a variational approach, which minimizes the harmonic energy. In this section, we will formulate the basic mathematical theory in a rigorous way. The harmonic energy and its derivative will be defined. Since we are working on a triangulated mesh, their discretized version will be discussed.

Let K represent the simplicial realization (triangulation) of a Riemann surface, u, v to dentote the vertices, and $[u, v]$ to denote the edge spanned by u, v. We use f, g to denote the piecewise linear function on K, $\vec{f}$ to represent vector valued functions.

Definition 2.1. All piecewise linear functions defined on K form a vector space, called $C^{PL}(K)$.

Definition 2.2. Suppose a set of string $k_{u,v}$ are assigned to each edge $[u, v]$. An inner product can be defined on $C^{PL}(K)$ as follow:

$$\langle f, g \rangle = \frac{1}{2} \sum_{[u,v] \in K} k_{u,v} \big(f(u) - f(v) \big) \big(g(u) - g(v) \big).$$

Definition 2.3. Suppose $f \in C^{PL}$. The string energy is defined as:

$$E(f) = \langle f, f \rangle = \frac{1}{2} \sum_{[u,v] \in K} k_{u,v} \big(f(u) - f(v) \big)^2.$$

Definition 2.4. Suppose edge $[v_1, v_2]$ has two adjacent faces T_α, T_β, with $T_\alpha = \{v_1, v_2, v_3\}$, $T_\beta = \{v_1, w_3, v_2\}$. Define the parameters

$$a^\alpha_{v_1, v_2} = \frac{(v_1 - v_3) \cdot (v_2 - v_3)}{2|(v_1 - v_3) \times (v_2 - v_3)|},$$

$$a^\alpha_{v_2, v_3} = \frac{(v_2 - v_1) \cdot (v_3 - v_1)}{2|(v_2 - v_1) \times (v_3 - v_1)|},$$

$$a^\alpha_{v_3, v_1} = \frac{(v_3 - v_2) \cdot (v_1 - v_2)}{2|(v_3 - v_2) \times (v_1 - v_2)|},$$

T_β is defined similarly. If $k_{v_1, v_2} = a^\alpha_{v_1, v_2} + a^\beta_{v_1, v_2}$, the string energy obtained is called the harmonic energy E_{harmonic}.

Definition 2.5. For a map $\vec{f} \in C^{PL}$, $\vec{f} = (f_0, f_1, f_2)$, we define the harmonic energy as:

$$E_{\text{harmonic}}(\vec{f}) = \sum_{i=0}^{2} E_{\text{harmonic}}(f_i).$$

---

[1] We adapted the harmonic energy computation in [4].

For a map between two genus zero surfaces, the map is conformal if the harmonic energy $E_{harmonic}$ is equal to zero. We can then deform a homeomorphism $\vec{f} : K \to S^2$ into a conformal mapping by minimizing the harmonic energy $E_{harmonic}(\vec{f})$.

3. Optimization of brain conformal parametrization

In this paper, we will describe two methods to adjust conformal parameterizations of the cortical surface so that they match consistent anatomical features across subjects. This matching of cortical patterns improves the alignment of data across subjects, e.g., when integrating functional imaging data across subjects, measuring brain changes, or making statistical comparisons in cortical anatomy [8]. In this section, two approaches will be discussed.

3.1. Optimal Möbius transformation

In this approach, we propose to optimize the conformal parametrization by compositing it with an optimal Möbius transformation which reduces the landmark mismatch error. We define an energy to measure the quality of the parameterization. Suppose two brain surfaces S_1, S_2 are given, conformal parameterizations are denoted as $f_1 : S^2 \to S_1$ and $f_2 : S^2 \to S_2$, we can define the matching energy as:

$$E(f_1, f_2) = \int\limits_{S^2} \left\| f_1(u, v) - f_2(u, v) \right\|^2 du \, dv.$$

We can compose an optimal Möbius transformation τ with f_2 which minimizes the matching energy. That is,

$$E(f_1, f_2 \circ \tau) = \min_{\zeta \in \Omega} E(f_1, f_2 \circ \zeta).$$

In order to match the important geometric features on the brains, landmarks are commonly used. Suppose the landmarks are represented as discrete point sets and denoted as $\{p_i \in S_1\}$ and $\{q_i \in S_2\}$, p_i matches q_i, $i = 1, 2, \ldots, n$. The landmark mismatch functionla for $u \in \Omega$ is as follow:

$$E(u) = \sum_{i=1}^{n} \left\| f_1^{-1}(p_i) - u \left(f_2^{-1}(q_i) \right) \right\|^2, \quad u \in \Omega, \ p_i \in S_1, \ q_i \in S_2.$$

We next convert the nonlinear variational problem into a least square problem. We project the sphere to the complex plane, then the Möbius transformation is represented as a complex linear rational formula. If we assume u maps infinity to infinity, then u can be represented in a linear form as $u = az + b$. Then $E(u)$ can be simplified as:

$$E(u) = \sum_{i=1}^{n} g(z_i) |az_i + b - \tau_i|^2,$$

where z_i is the stero-projection of p_i, τ_i is the projection of q_i, g the conformal factor from the plane to the sphere which can be simplified as:

$$g(z) = 4 / \left(1 + |z|^2 \right).$$

The problem becomes a least squares problem.

This algorithm allows us to produce an optimal map that preserves exactly the conformality. However, since this method minimizes the energy with respect to the six degree of freedom of the Möbius transformation group, the minimization of the landmark mismatch error is not as effective as our second approach, the variational approach, which will be discussed in the next section.

3.2. Variational approach

Our second method, which is based on a new energy functional, optimizes the conformal parameterization of cortical surfaces by using landmarks. This is done by minimizing the compound energy functional $E_{new} = E_{harmonic} + \lambda E_{landmark}$, where $E_{harmonic}$ is the harmonic energy of the parameterization and $E_{landmark}$ is the landmark mismatch

energy. We prove theoretically that our proposed E_{new} is guaranteed to be decreasing and studied the rate of changes of $E_{harmonic}$ and $E_{landmark}$. Experimental results show that our algorithm can considerably reduce the landmark mismatch energy while effectively retaining the conformality property. Based on these findings, we argue that the conformal mapping provides an attractive framework to help analyze anatomical shape, and to statistically combine or compare 3D anatomical models across subjects.

We now propose a variational approach that optimizes the conformal parameterization using discrete landmarks. This algorithm optimizes the landmark mismatch energy over all degrees of freedom in the reparameterization group. The map obtained can considerably reduce the landmark mismatch energy while retaining conformality as far as possible.

Suppose C_1 and C_2 are two cortical surfaces we want to compare. We let $f_1 : C_1 \rightarrow S^2$ be the conformal parameterization of C_1 mapping it onto S^2. We manually label the landmarks on the two cortical surfaces as discrete point sets, as shown in Fig. 1. We denote them as $\{p_i \in C_1\}$, $\{q_i \in C_2\}$, with p_i matching q_i. We proceed to compute a map $f_2 : C_2 \rightarrow S^2$ from C_2 to S^2, which minimizes the harmonic energy as well as minimizing the so-called landmark mismatch energy. The landmark mismatch energy measures the Euclidean distance between the corresponding landmarks. Note that it makes sense to use Euclidean distance instead of geodesic distance. On $\mathbb{S}^2$, all the geodesic curves move along the great circle. As the Euclidean distance decreases, the geodesic distance will also decrease. In other words, the computed map should effectively preserve the conformal property and match the geometric features on the original structures as far as possible.

Let $h : C_2 \rightarrow S^2$ be any homeomorphism from C_2 onto S^2. We define the landmark mismatch energy of h as, $E_{landmark}(h) = 1/2 \sum_{i=1}^{n} \|h(q_i) - f_1(p_i)\|^2$, where the norm represents distance on the sphere. By minimizing this energy functional, the Euclidean distance between the corresponding landmarks on the sphere is minimized.

To optimize the conformal parameterization, we propose to find $f_2 : C_2 \rightarrow S^2$ which minimizes the following new energy functional (instead of the harmonic energy functional), $E_{new}(f_2) = E_{harmonic}(f_2) + \lambda E_{landmark}(f_2)$, where λ is a weighting factor (Lagrange multiplier) that balances the two penalty functionals. It controls how much landmark mismatch we want to tolerate. When $\lambda = 0$, the new energy functional is just the harmonic energy. When λ is large, the landmark mismatch energy can be significantly reduced. But more conformality will be lost (here we regard deviations from conformality to be quantified by the harmonic energy).

Now, let K represent the simplicial realization (triangulation) of the brain surface C_2, let u, v denote the vertices, and $[u, v]$ denote the edge spanned by u, v. Our new energy functional can be written as:

$$E_{new}(f_2) = \frac{1}{2} \sum_{[u,v] \in K} k_{u,v} \|f_2(u) - f_2(v)\|^2 + \frac{\lambda}{2} \sum_{i=1}^{n} \|f_2(q_i) - f_1(p_i)\|^2$$
$$= \frac{1}{2} \sum_{[u,v] \in K} k_{u,v} \|f_2(u) - f_2(v)\|^2 + \frac{\lambda}{2} \sum_{u \in K} \|f_2(u) - L(u)\|^2 \chi_M(u),$$

where $M = \{q_1, \ldots, q_n\}$; $L(q_i) = p_i$ if $u = q_i \in M$ and $L(u) = (1, 0, 0)$ otherwise. The first part of the energy functional is defined as in [4]. Note that by minimizing this energy, we may give up some conformality but the landmark mismatch energy is progressively reduced.

3.3. Optimization of combined energy

We next formulate a technique to optimize our energy functional. Suppose we would like to compute a mapping f_2 that minimizes the energy $E_{new}(f_2)$. This can be solved easily by steepest descent.

Definition 3.1. Suppose $f \in C^{PL}$, where C^{PL} represent a vector space consists of all piecewise linear functions defined on K. We define the Laplacian as follows: $\Delta f(u) = \sum_{[u,v] \in K} k_{u,v}(f(u) - f(v)) + \lambda \sum_{u \in K} (f_2(u) - L(u)) \chi_M(u)$.

Definition 3.2. Suppose $\vec{f} \in C^{PL}$, $\vec{f} = (f_0, f_1, f_2)$, where the f_i are piecewise linear. Define the Laplacian of $\vec{f}$ as $\Delta \vec{f} = (\Delta f_0(u), \Delta f_1(u), \Delta f_2(u))$.

Now, we know that $f_2 = (f_{20}, f_{21}, f_{22})$ minimizes $E_{new}(f_2)$ if and only if the tangential component of $\Delta f_2(u) = (\Delta f_{20}(u), \Delta f_{21}(u), \Delta f_{22}(u))$ vanishes. That is $\Delta(f_2) = \Delta(f_2)^{\perp}$.
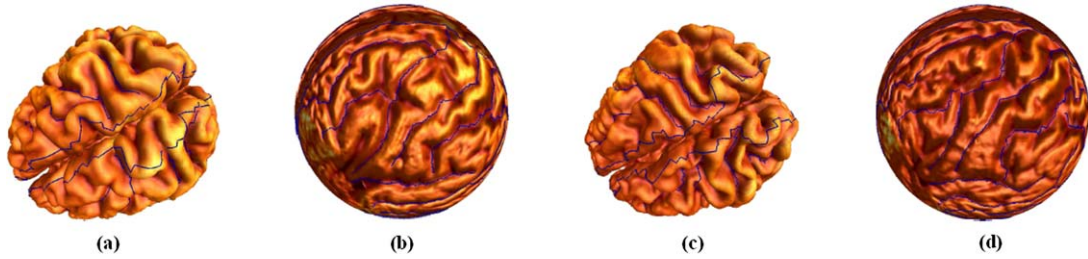
Fig. 3. Möbius transformation to minimize the landmark mismatch error. The blue curve represented the important landmarks. Note that the alignment of sulci landmarks is quite consistent. (For interpretation of the references in colour in this figure legend, the reader is referred to the web version of this article.)

In other words, we should have $P_{\vec{n}}\Delta f_2(u) = \Delta f_2(u) - (\Delta f_2(u) \cdot \vec{n})\vec{n} = 0$. We use a steepest descent algorithm to compute $f_2 : C_2 \to S^2 : \frac{df_2}{dt} = -P_{\vec{n}}\Delta f_2(t)$.

Algorithm 1. *Algorithm to optimize the combined energy E_{new} input (mesh K, step length δt, energy difference threshold δE), output ($f_2 : C_2 \to S^2$), which minimizes E. The computer algorithm proceeds as follows*:

(1) *Given a Gauss map $I : C_2 \to S^2$. Let $f_2 = I$, compute $E_0 = E_{\text{new}}(I)$;*
(2) *For each vertex $v \in K$, compute $P_{\vec{n}}\Delta f_2(v)$;*
(3) *Update $f_2(v)$ by $\delta f_2(v) = -P_{\vec{n}}\Delta f_2(v)\delta t$;*
(4) *Compute energy E_{new};*
(5) *If $E_{\text{new}} - E_0 < \delta E$, return f_2. Otherwise, assign E to E_0. Repeat steps 2 to 5.*

4. Experimental results

In our experiment, we tested our algorithm on a set of left hemisphere cortical surfaces generated from brain MRI scans of 40 healthy adult subjects, aged $27.5 +/- 7.4$SD years (16 males, 24 females), scanned at 1.5 T (on a GE Signa scanner). Data and cortical surface landmarks were those generated in a prior paper, Thompson et al. [8] where the extraction and sulcal landmarking procedures are fully detailed. Using this set of 40 hemispheric surfaces, we mapped all surfaces conformally to the sphere and optimized the conformal map by the two approaches. In our first approach, we optimized the conformal map by composing it with an optimal Möbius transformation, which reduced the landmark mismatch error. Note that the optimized maps we get remains exactly conformal. Fig. 3 shows some of our experimental result. Note that the alignment of sulci landmarks are quite consistent after optimizing the map with the optimal Möbius transformation.

In our second approach, we mapped the cortical surfaces conformally to the sphere and minimized the compound energy matching all subjects to a randomly selected individual subject (alternatively, the surfaces could have been aligned to an average template of curves on the sphere). An important advantage of this approach is that the local adjustments of the mapping to match landmarks do not greatly affect the conformality of the mapping. In Fig. 4(a), the cortical surface C_1 (a control subject) is mapped conformally ($\lambda = 0$) to the sphere. In (b), another cortical surface C_2 is mapped conformally to the sphere. Note that the sulcal landmarks appear very different from those in (a) (see landmarks in the green square) (for colours see the web version of this article). This means that the geometric features are not well aligned on the sphere unless a further feature-based deformation is applied. In Fig. 4(c), we map the cortical surface C_2 to the sphere with our algorithm, while minimizing the compound energy. This time, the landmarks closely resemble those in (a) (see landmarks in the green square).

In Fig. 5, statistics of the angle difference are illustrated. Note that under a conformal mapping, angles between edges on the initial cortical surface should be preserved when these edges are mapped to the sphere. Any differences in angles can be evaluated to determine departures from conformality. Fig. 5(a) shows the histogram of the angle difference using the conformal mapping, i.e. after running the algorithm using the conformal energy term only. Fig. 4(b) shows the histogram of the angle difference using the compound functional that also penalizes landmark mismatch. Despite the fact that inclusion of landmarks requires more complex mappings, the angular relationships between edges
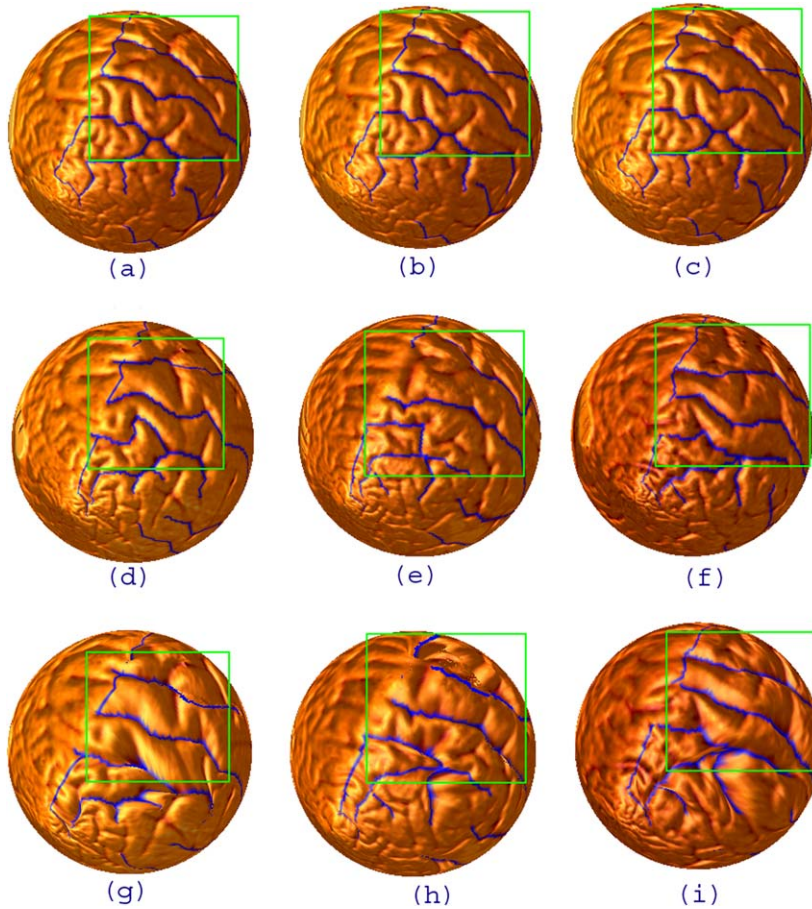
Fig. 4. In (a), the cortical surface C_1 (the control) is mapped conformally ($\lambda = 0$) to the sphere. In (d), another cortical surface C_2 is mapped conformally to the sphere. Note that the sulcal landmarks appear very different from those in (a) (see landmarks in the green square). In (g), the cortical surface C_2 is mapped to the sphere using our algorithm (with $\lambda = 3$). Note that the landmarks now closely resemble those in (a) (see landmarks in the green square). (b) and (c) shows the same cortical surface (the control) as in (a). In (e) and (f), two other cortical surfaces are mapped to the spheres. The landmarks again appears very differently. In (h) and (i), the cortical surfaces are mapped to the spheres using our algorithm. The landmarks now closely resemble those of the control. (For interpretation of the references in colour in this figure legend, the reader is referred to the web version of this article.)
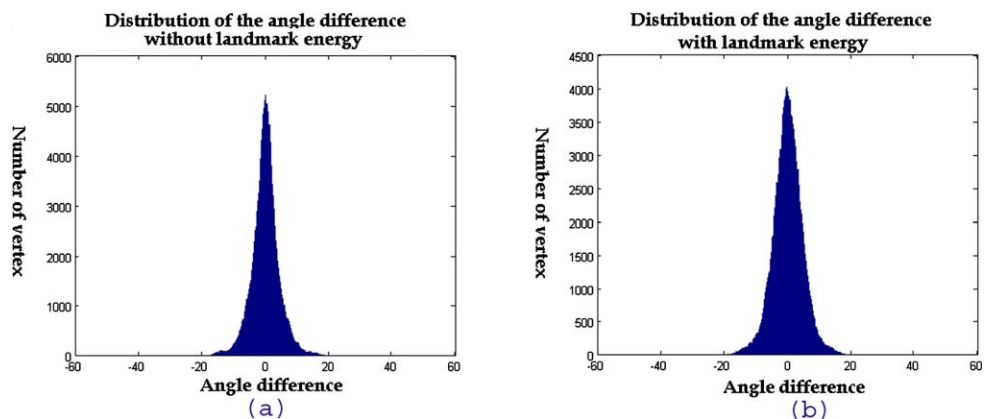
Fig. 5. Histogram (a) shows the statistics of the angle difference using the conformal mapping. Histogram (b) shows the statistic of the angle difference using our algorithm ($\lambda = 3$). It is observed that the angle is significantly preserved.
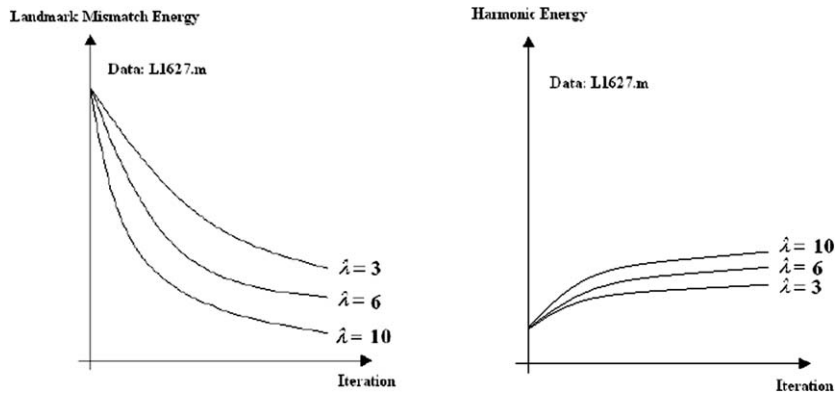
Fig. 6. Diagram that shows how the harmonic energy and landmark mismatch energy change at each iteration. The left shows how the landmark mismatch energy changes. The right shows how the harmonic energy changes.
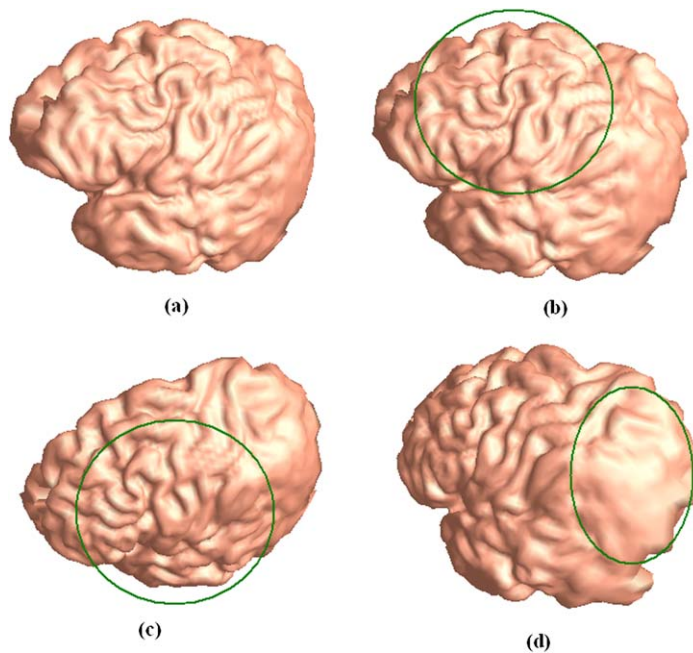
Fig. 7. The average map of the optimized conformal parametrization using the variational approach. 40 landmarks are manually labelled. Observed that the important sulci landmarks are clearly shown. It means that the landmarks are consistently aligned.

on the source surface and their images on the sphere are clearly well preserved even after landmark constraints are enforced.

In Fig. 9, statistic of the percentage change in the conformal factor are illustrated. The left shows the percentage change in the conformal factor using the variational approach with $\lambda = 3$. The right shows the percentage change in the conformal factor using the variational approach with $\lambda = 6$. Note that the conformality is well preserved. However, more percentage change in conformality is observed with larger λ.

We also tested with other parameter λ with different values. Table 1 shows numerical data from the experiment. From Table 1, we observe that the landmark mismatch energy is significantly reduced while the harmonic energy is only slightly increased. Table 1 also illustrates how the results differ with different values of λ. We observe that the landmark mismatch error can be reduced by increasing λ, but conformality is increasingly lost. Fig. 6 shows how the harmonic energy and landmark energy change in each iterations with different values of λ. Again, more landmark mismatch error can be reduced with larger λ, but more harmonic energy (the conformality) is lost.

Mobius Transformation   **Variational Method with** $\lambda = 6$

(40 landmarks added)
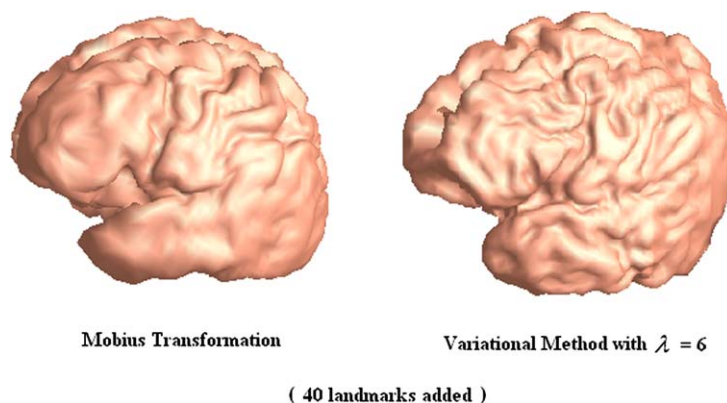
Fig. 8. The average map of the optimized conformal parametrization by the two different approaches.
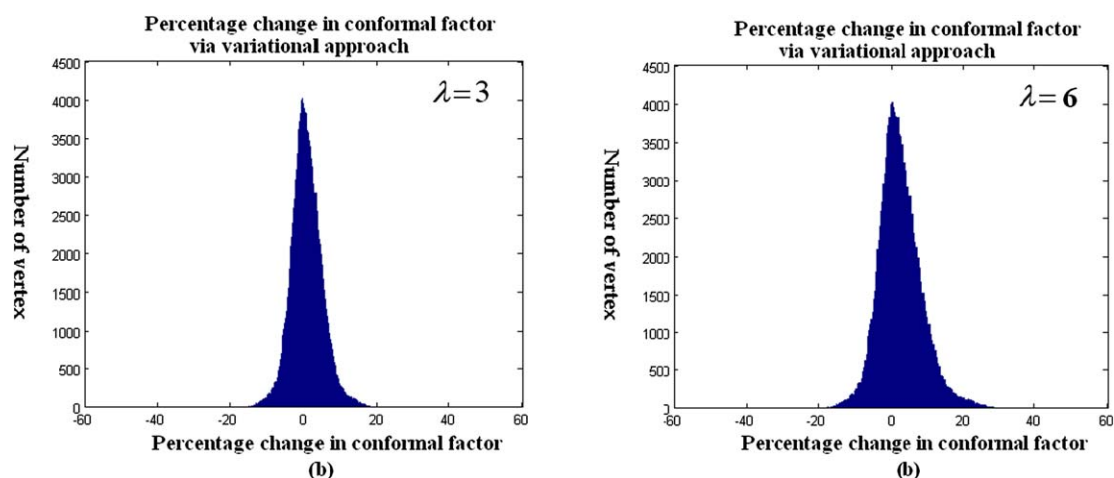
Fig. 9. Histogram showing the percentage change in the conformal factor with different algorithm. The left shows the percentage change in the conformal factor using the variational approach with $\lambda = 3$. The right shows the percentage change in the conformal factor using the variational approach with $\lambda = 6$. Note that the conformality is well preserved. However, more conformality will be lost with larger λ.

Table 1
Numerical data from our experiment. The landmark mismatch energy is significantly reduced while the harmonic energy is only slightly increased. The table also illustrates how the results differ with different values of λ. The landmark mismatch error can be reduced by increasing λ, but conformality will increasingly be lost

	$\lambda = 3$	$\lambda = 6$	$\lambda = 10$
E_{harmonic} of the initial (conformal) parameterization:	100.6	100.6	100.6
$\lambda E_{\text{landmark}}$ of the initial (conformal) parameterization:	81.2	162.4	270.7
Initial compound energy ($E_{\text{harmonic}} + \lambda E_{\text{landmark}}$):	181.8	263.0	371.3
Final E_{harmonic}	109.1 ($\nearrow$ 8.45%)	111.9 ($\nearrow$ 11.2%)	123.0 ($\nearrow$ 22.2%)
Final $\lambda E_{\text{landmark}}$	11.2 ($\searrow$ 86.2%)	13.7 ($\searrow$ 91.6%)	15.6 ($\searrow$ 95.8%)
Final compound energy ($E_{\text{harmonic}} + \lambda E_{\text{landmark}}$)	120.3 ($\searrow$ 33.8%)	125.6 ($\searrow$ 52.2%)	138.6 ($\searrow$ 62.7%)

To visualize how well the alignment of the important sulci landmarks is, we took average of the 15 optimized maps using the variational method. Fig. 7 shows average maps at different angles (for colours see the web version of this article). In (b) and (c), sulci landmarks are clearly preserved inside the green circle where landmarks are manually labelled. In (d), the sulci landmarks are averaged out inside the green circle where no landmarks are manually labelled. It means that our algorithm can significantly improve the alignment of the anatomical features.

Table 2

Numerical data from our experiment of the two different approaches. Although the Möbius transformation approach generate a map which is conformal, the landmark mismatch energy is not reduced as effective as the variational approach. The landmark mismatch energy is significantly reduced with the variational approach. The table also illustrates how the results differ with different values of λ. The landmark mismatch error can be reduced by increasing λ, but conformality will increasingly be lost

	Möbius transformation	Variational $\lambda = 3$	Variational $\lambda = 6$
E_{landmark} of the initial (conformal) parameterization:	160.33	160.33	160.33
E_{landmark} of the final (optimized) parameterization:	73.75	19.24	9.62

Note that our first algorithm is different from the second one in that the first method can generate an optimized map which remains exactly conformal, although the reduction in the landmark mismatch error is not as effective as the second approach. Table 2 shows the numerical data of our experiment. From Table 2, we observe that the variational method can reduce the landmark mismatch error more effectively than the optimal Möbius transformation approach. It is also observed that more landmark mismatch can be reduced by larger value of λ. Fig. 8 shows the average maps of the optimized conformal maps we got by the two different approaches. Fig. 8(a) shows the average maps of the optimal Möbius transformation approach. Fig. 8(b) shows the average map of the variational approach. Note that the sulci landmarks are better preserved using the variational approach.

5. Conclusion and future work

In conclusion, we have described two algorithms to compute a map from the cortical surface of the brain to a sphere, which can effectively match consistent anatomical features across subjects. This is done by minimizing the landmark mismatch error across different subjects. The landmark mismatch error measures the distance between the corresponding landmarks. The first method, which is based on the optimal Möbius transformation, can generate an optimal map that is exactly conformal. However, the landmark mismatch error is not reduced as significant as the second approach. Our second method is a variational approach which minimizes a compound energy. The compound energy functional consists of the harmonic energy and the landmark mismatch energy with adjustable landmark weights. The harmonic energy in the energy functional determines how much conformality we want to preserve, whereas the landmark energy determines how much landmark mismatch error we can tolerate. The development of adjustable landmark weights may be beneficial in computational anatomy, too. In some applications, such as tracking brain change in an individual over time, in serial images, it makes most sense to place a high priority on landmark correspondence. In other applications, such as the integration of functional brain imaging data across subjects, functional anatomy is not so tightly linked to sulcal landmarks, so it may help to trade landmark error to increase the regularity of the mappings. In the future, we will study the numerical parameters of our algorithm in details to determine how the weighting factor λ affects the signal to noise for different neuroimaging applications. We will also compare our algorithm with other existing counterpart quantitatively. Furthermore, more analysis will be done to examine how well the alignment of the sulci/gyri is, such as averaging the maps.

Summary

Developing an effective way to compare and integrate brain data has long been a challenging problem in the brain mapping research. One typical way to do it is to map data from multiple subjects into a canonical space. Usually, cortical surfaces are mapped conformally onto the sphere without angular distortion, generating an orthogonal grid on the cortex that locally preserves the metric. Although conformal mapping preserves the local geometry well, the important anatomical features, such as the sulci landmarks, are usually not aligned consistently. To compare cortical surfaces more effectively, it is advantageous to adjust the conformal parameterizations to match consistent anatomical features across subjects. In this paper, we propose a new framework which combines genus zero surface conformal mapping with some explicit constraints. The constraints are generally geometric feature based. The framework has the advantages that the constrain energy is dramatically reduced while the conformalilty is significantly kept. Right now, we mainly apply these frameworks to the brain surface mapping research. In the future, we will look for some broader applications.
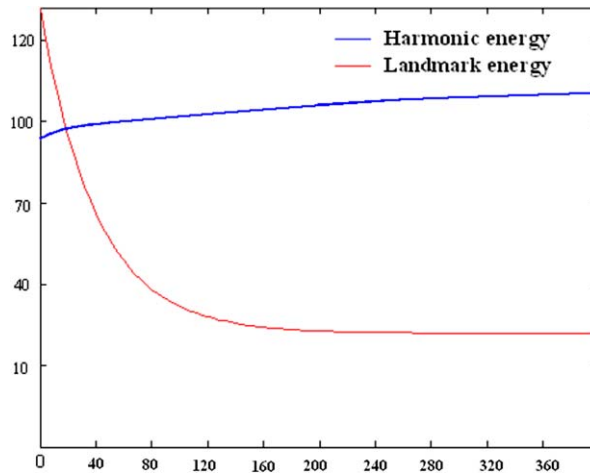
Fig. 10. This figure shows how the harmonic energy and landmark energy change, as the number of iterations increases, using our steepest descent algorithm. Initially, the rate of change of the harmonic energy is small while the rate of change of landmark energy is comparatively large. Note that a Lagrange multiplier governs the weighting of the two energies, so a compromise can be achieved between errors in landmark correspondence and deviations from conformality.

Appendix A. Energy is decreasing

Claim. *With our algorithm, the energy is strictly decreasing.*

Proof. Our energy (in continuous form) can be written as: $E(u) = 1/2 \int \|\nabla u\|^2 + \lambda \int \delta_E \|(u - v)\|^2$ where v is the conformal mapping from the control cortical surface to the sphere and $\delta_E(x)$ is the smooth approximation of the characteristic function:

$$\chi_E(x) = \begin{cases} 1 & \text{if } x \text{ is a landmark point,} \\ 0 & \text{else.} \end{cases}$$

Now, $\frac{d}{dt}|_{t=0} E(u + tw) = \int \nabla u \cdot \nabla w + \lambda \int \delta_E (u - v) \cdot w = -\int \Delta u w + \lambda \int \delta_E (u - v) \cdot w$ In our algorithm, the direction w is taken as: $w = \Delta u - \lambda \delta_E (u - v)$. Substituting this into the above equation, we have $\frac{d}{dt}|_{t=0} E(u + tw) = -\int (\nabla u)^2 - (\lambda)^2 \int \delta_E \|u - v\|^2 < 0$. Therefore, the overall energy of the mapping is strictly decreasing, as the iterations proceed. $\square$

Appendix B. Rate of changes in E_{harmonic} and E_{landmark}

To explain why our algorithm can effectively preserve conformalilty while greatly reducing the landmark mismatch energy, we can look at the rate of change of E_{harmonic} and E_{landmark}. Note that the initial map u we get is almost conformal. Thus, initially Δu is very small.

Claim. *With our algorithm, the rate of change of $E_{\text{harmonic}}(u)$ is $\mathcal{O}(\|\Delta u\|_\infty)$ and the rate of change of E_{landmark} is $\lambda^2 E_{\text{landmark}}(u) + \mathcal{O}(\|\Delta u\|_\infty)$. Here the norm is the supremum norm over the surface.*

Proof. Recall that in our algorithm, the direction w is taken as: $w = \Delta u - \lambda \delta_E (u - v)$. Now, the rate of changes are

$$\begin{aligned} E_{\text{harmonic}} &= \left| \frac{d}{dt} \Big|_{t=0} E_{\text{harmonic}}(u + tw) \right| = \left| \int \nabla u \cdot \nabla w \right| = \left| \int \Delta u \cdot w \right| \\ &= \left| \int \|\Delta u\|^2 + \lambda \int \delta_E \Delta u \cdot (u - v) \right| \\ &\quad \times \left[\text{since the area of the unit sphere is } 4\pi \text{ and } \|u - v\|_\infty \leqslant 2 \right] \\ &\leqslant \|\Delta u\|_\infty^2 + 8\lambda \pi \|\Delta u\|_\infty = \mathcal{O}\big(\|\Delta u\|_\infty\big), \end{aligned}$$

$$E_{\text{landmark}} = \left| \frac{d}{dt} \Big|_{t=0} E_{\text{landmark}}(u + tw) \right|$$

$$= \left| \int (\lambda \delta_E)^2 \|u - v\|^2 + \lambda \int \delta_E (u - v) \cdot \Delta u \right|$$

$$\leqslant \lambda^2 E_{\text{landmark}}(u) + 8\lambda \pi \|\Delta u\|_\infty$$

$$\times \left[\text{since the area of the unit sphere is } 4\pi \text{ and } \|u - v\|_\infty \leqslant 2 \right]$$

$$\times \left(\geqslant \lambda^2 E_{\text{landmark}}(u) + C \|\Delta u\|_\infty, \text{ for some constant } C \right)$$

$$= \lambda^2 E_{\text{landmark}}(u) + \mathcal{O}\left(\|\Delta u\|_\infty \right).$$

Since initially the map is almost conformal and Δu is very small, the change in harmonic energy is very small. Conversely, initially the landmark energy is comparatively large. Since the rate of change of E_{landmark} is $\lambda^2 E_{\text{landmark}}(u) + C \|\Delta u\|_\infty$, the change in landmark energy is more significant (see Fig. 10 for an illustration). □

References

[1] H. Drury, D.V. Essen, M. Corbetta, A. Snyder, Surface-based analyses of the human cerebral cortex, in: Brain Warping, Academic Press, San Diego, 1999, pp. 337–363.

[2] B. Fischl, M. Sereno, R. Tootell, A. Dale, High-resolution intersubject averaging and a coordinate system for the cortical surface, Human Brain Mapping 8 (1999) 272–284.

[3] J. Glaunès, M. Vaillant, M. Miller, Landmark matching via large deformation diffeomorphisms on the sphere, J. Math. Imaging Vision 20 (2004) 179–200.

[4] X. Gu, Y. Wang, T. Chan, P. Thompson, S.T. Yau, Genus zero surface conformal mapping and its application to brain surface mapping, IEEE Trans. Med. Imaging 23 (2004) 949–958.

[5] S. Haker, S. Angenent, A. Tannenbaum, R. Kikinis, G. Sapiro, M. Halle, Conformal surface parameterization for texture mapping, IEEE TVCG 6 (2000) 181–189.

[6] M.K. Hurdal, K. Stephenson, Cortical cartography using the discrete conformal approach of circle packings, NeuroImage 23 (2004) S119–S128.

[7] A. Leow, C. Yu, S. Lee, S. Huang, R. Nicolson, K. Hayashi, H. Protas, A. Toga, P. Thompson, Brain structural mapping using a novel hybrid implicit/explicit framework based on the level-set method, NeuroImage 24 (2005) 910–927.

[8] P. Thompson, et al., Mapping cortical change in alzheimer's disease, brain development, and schizophrenia, NeuroImage 23 (2004) S2–S18.

[9] P. Thompson, R. Woods, M. Mega, A. Toga, Mathematical/computational challenges in creating population-based brain atlases, Human Brain Mapping 9 (2000) 81–92.

[10] B. Timsari, R.M. Leahy, Optimization method for creating semi-isometric flat maps of the cerebral cortex, Proc. SPIE (3979) 698–708.

[11] D. Tosun, M. Rettmann, J. Prince, Mapping techniques for aligning sulci across multiple brains, Med. Image Anal. 8 (2004) 295–309.

[12] Y. Wang, X. Gu, K. Hayashi, T. Chan P. Thompson, S.T. Yau, Brain surface parameterization using riemann surface structure, in: 8th International Conference on Medical Image Computing and Computer Assisted Intervention (MICCAI), 2005.